Bioresource Technology 388 (2023) 129675

Contents lists available at ScienceDirect

Bioresource Technology

journal homepage: www.elsevier.com/locate/biortech

Effect of different types of volatile fatty acids on the performance and bacterial population in a batch reactor performing biological nutrient removal

Ruby Diaz, Soklida Hong, Ramesh Goel *

Department of Civil and Environmental Engineering, University of Utah, Salt Lake City, UT 84112, USA

HIGHLIGHTS

- Four different volatile fatty acids were used for sustainable biological nutrient removal.
- High concentrations of acetic acid appear to benefit the proliferation of *Defluviicoccus*.
- Valeric acid, commonly found in fermented sludge, appear to benefit nitrification.
- The presence of VFAs with high molecular weight indicated to benefit denitrification.
- DPAO capable of using nitrite as electron acceptor belonging to Clade IIC were existent.

GRAPHICAL ABSTRACT

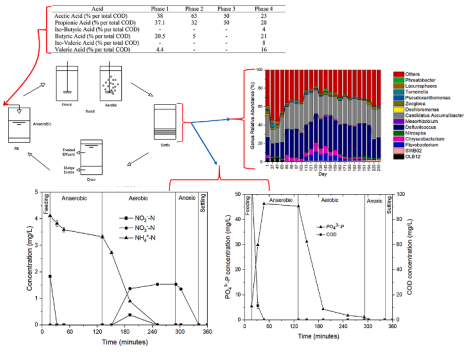

ARTICLE INFO

Keywords:
BNR
Sludge fermentation
Volatile fatty acids
Candidatus Accumulibacter
Defluviicoccus

ABSTRACT

Different ratios of four volatile fatty acids (VFAs) were used as the primary feed to a laboratory scale biological nutrient reactor during four operational stages. The reactor performed efficiently over 500 days of operation with over 90% dissolved phosphorus and over 98% ammonium-nitrogen (NH_4^+-N) removal. Through in the first experimental phase, acetate and propionate were present in a significant proportion as carbon sources, the relative abundance of *Candidatus* Accumulibacter, a potential polyphosphate accumulating organism, increased from 10% to 57% and the *Defluviicoccus* genus, a known glycogen accumulating organism (GAO), decreased from 41% to 5%. Further tests indicated the presence of denitrifying phosphorus accumulating organisms (DPAO) belonging to Clade IIC, that could use nitrite as the electron acceptor during P-uptake. In general, VFAs favored the increase of the genus *Defluviicoccus* and *Candidatus* Accumulibacter. High relative abundance of *Defluviicoccus* did not affect the stability and the performance of the BNR process.

1. Introduction

The anthropogenic phosphorus loadings from point and nonpoint sources to freshwater bodies have been estimated to be 1.5 Tg/year, of which 54% originates from domestic sources, 38% from agriculture, and the remaining 8% from industrial sources. Municipal and industrial

* Corresponding author.
E-mail address: ram.goel@utah.edu (R. Goel).

https://doi.org/10.1016/j.biortech.2023.129675
Received 3 April 2023; Received in revised form 7 August 2023; Accepted 10 August 2023
Available online 23 August 2023

wastewater treatment plants (WWTPs) situated in urban areas have become major contributors of nitrogen and phosphorus to surrounding water bodies. In the United States, over 50% of nutrient influx to rivers, lakes and streams located in urbanized areas comes from point sources. Excessive nutrient loading in aquatic environments has shown to cause eutrophication which results in low dissolved oxygen (DO) in water, causes fish mortality, increases turbidity, and can enhance toxic algal blooms. Nitrogen present in the form of ammonia, nitrite, or nitrate is another nutrient present in wastewaters that can have detrimental effects on aquatic ecosystems with the most common pollutant being discharged into water streams being ammonia.

Chemical, physical and biological are generally used to manage dissolved P in liquid waste streams but biological treatment has emerged as an inexpensive and sustainable method that uses bacteria naturally found in waste streams to remove phosphorus, nitrogen, and COD through the use of various metabolic processes (Rout et al., 2021). In biological treatment, the removal of phosphorus is achieved by microorganisms known as phosphorus accumulating organisms or PAOs. Conventionally, nitrification is performed by ammonium oxidizing bacteria (AOB) followed by nitrite-oxidizing bacteria (NOB) and the recently discovered commamox (complete oxidation of ammonium to nitrate by single organism) organisms. Denitrification is performed by ordinary heterotrophic organisms which typically require external carbon sources (Rout et al., 2021). Another group of microorganisms identified in the last 15 years that can perform simultaneous phosphorus uptake and denitrification, are denitrifying phosphorus accumulating organisms or (DPAOs). DPAOs assimilate volatile fatty acids (VFAs) in the anaerobic phase and incorporate them intracellularly as poly-β-hydroalkanoate (PHA), and use this intracellular PHA as a carbon source later throughout the anoxic phase (Zeng et al., 2016). Nitrification is performed under aerobic or microaerobic conditions where AOBs oxidize the ammonia present to nitrite and NOBs oxidize the produced nitrite to nitrate.

Many wastewater treatment plants have weak influent wastewaters with COD $\leq$ 250 mg/L, and reduction on the concentration of organic material present in WWTPs have been observed during wet periods. A link between low organic loadings and the loss and/or decrease in enhanced biological phosphorus removal (EBPR) was recorded by Okada et al., 1992. Carbon sources that contain readily biodegradable chemical oxygen demand (rbCOD) such as VFAs, are needed to maintain removal of nitrogen and phosphorus. Sludge fermentation has been identified as a reliable and efficient method to generate VFAs to support biological nutrient removal (BNR) processes (Chen et al., 2021). On-site VFAs production through sludge fermentation provides carbon neutrality and reduction in excess sludge which would otherwise need further handling and processing. The main VFAs generated during the fermentation of municipal wastewater are acetic, propionic, butyric, *iso*-butyric, valeric and *iso*-valeric. (Owusu-Agyeman et al., 2020). Although, literature reports the use and the effect of different VFAs on EBPR process performance, studies have been limited on the effect of all major VFAs which could potentially generate during sludge fermentation and the effect of their changing ratio on BNR performance and microbiology. This study incorporates the use of four different VFAs mixtures. One of the mixtures included a combination of the main VFAs typically found during fermentation of primary and secondary sludge. This projects analyzed how different VFAs ratios affected the performance of the reactor and tracked changes in bacteria communities. Four different VFAs combinations were evaluated, with Phase I, representing the acetic percentage produced from the fermentation of waste-activated sludge (Vidal-Antich et al., 2021). Phase II representing the acetic ratio obtained from sludge fermentation from an aeration tank with heat alkaline treatment (Tan et al., 2012). Phase III representing the two main acids produced during the anaerobic fermentation of primary sludge (Li et al., 2017). Phase IV, the VFA mix, representing acids obtained from co-digesting primary and secondary sludge (Diaz et al., 2023). The reactor was run under anaerobic/aerobic/anoxic cycles. The main form of VFAs generated during sludge fermentation are acetic and propionic acids but other acids are also generated; the relative distribution of which depends on operational conditions (e.g. temperature, sludge age) and the microbial community. The idea behind using different ratios of VFAs was to simulate situations where sludge fermentation could behave differently and generate these VFAs in different concentrations. The approach included operating a lab scale at different VFA ratios to simulate varying fermentation outputs, monitoring the performance of the reactor including, nitrogen and P removal, measuring intracellular polymers in PAOs and monitoring the microbial ecology.

2. Materials and methods

2.1. Reactor operation

A laboratory-scale plexiglass cylindrical reactor operated in batch mode with a volume of 2 L and an inside diameter of 12.7 cm with a plexiglass cover served as the lab scale sequencing batch reactor (SBR). The inoculum used to seed the reactor was the return-activated sludge collected from the secondary clarifiers located at the Central Valley Water Reclamation Facility located in Salt Lake City, Utah. The reactor was operated at an ambient temperature of 21 $\pm$ 1 °C and had four 6-hour long cycles per day. Each cycle started with an anaerobic phase that lasted 2 h and 10 min, followed by an aerobic phase that lasted 2 h and 40 min, followed by an anoxic phase which operated for 50 min, with 18 min of settling time and ending with 2 min of decanting. During the anaerobic and anoxic phase, nitrogen was purged into the reactor to maintain an oxygen-free environment. During the aerobic phase, air was pumped into the reactor to maintain aerobic conditions. Feed was pumped into the reactor 10 min after the anaerobic phase started using a Masterflex L/S 20–600 rpm pump. The feed included 10 mL of 0.2 M solution of VFAs combined with 560 mL of synthetic wastewater mix. The hydraulic retention time (HRT) in the reactor was set to 20 h and a sludge retention time of 20 days. A Cole-Parmer pH probe 27020–06 was employed to monitor the pH which was kept between 7.4 and 7.8 by adding 0.25 (N) sodium hydroxide (NaOH) or 0.25 (N) sulfuric acid (H_2SO_4).

The pH in the reactor was controlled using an automatic pH controller manufactured by Cole-Parmer pH/ORP 300. Masterflex C/L 60 rpm pumps were used to pump the acid, base, and VFAs into the reactor. An electronic programmable timer and controller was used to control all the electrical components. The controller was manufactured by ChronTrol. During the anaerobic, aerobic, and anoxic phases, a Cimarec magnetic stirrer set at 125 rpm was used to stir the reactor. The reactor was analyzed during four different phases. During each phase, different combinations of VFAs were fed to the reactor. See Table 1 for VFA combinations used during the four different experimental phases. A stock solution of 1 M solution of VFAs was prepared in each phase at a concentration of 18,683 g of COD per litter of Milli-Q water. A working stock solution of 0.2 M of VFAs was prepared from this master stock solution using DI water and 10 mL of this solution was fed to the reactor at the beginning of the anaerobic phase. The feed recipe was adopted from Goel and Noguera (2006).

Each liter of the concentrated synthetic feed stock solution was

Table 1
VFAs percentage combinations for BNR reactor.

Acid	Phase 1	Phase 2	Phase 3	Phase 4
Acetic Acid (% per total COD)	38	63	50	23
Propionic Acid (% per total COD)	37.1	32	50	28
Iso-Butyric Acid (% per total COD)	–	–	–	4
Butyric Acid (% per total COD)	20.5	5	–	21
Iso-Valeric Acid (% per total COD)	–	–	–	8
Valeric Acid (% per total COD)	4.4	–	–	16

prepared using DI water and contained 2.26 g of NH4Cl, 1.72 g of CaCl2·.2H2O, 6.86 g of MgCL2.6H2) and 0.92 g of KH2PO4 and 30 mL of trace mineral solution. The recipe of the mineral stock was taken from Goel and Noguera (2006). A sodium bicarbonate (NaHCO3) stock solution was prepared at a concentration of 60 g/L. The influent was prepared as follows; for every liter of DI water fed to the reactor, 15.67 mL of sodium bicarbonate and 51.76 mL of synthetic wastewater stock solutions were added along with 10 mL of 0.2 M VFAs and 560 mL of influent feed at the beginning of each cycle. The VFAs stock solution was prepared to one mole of VFAs solution in 1L of DI water. Four different VFAs combinations were evaluated, with Phase I, representing the acetic and propionic acid percentage produced from the fermentation of waste-activated sludge (Luo et al., 2020; Vidal-Antich et al., 2021). Phase II represents the ratio obtained from sludge fermentation from an aeration tank with heat alkaline treatment (Tan et al., 2012). Phase III represents the two main acids produced during the anaerobic fermentation of primary sludge (Li et al., 2017). Phase IV, the VFA mix, represents acids obtained from co-digesting primary and secondary sludge (Diaz et al., 2023).

2.2. Analytical methods

Total (TSS) and volatile suspended solids (VSS) were measured using the protocol in 2005 standard method APHA-AWWA-WPCF. As soon as the samples were taken from the reactor, a syringe filter with 0.22 μm pore size, PES, 25 mm, manufactured by Thermo scientific was used to filter them. COD concentrations were estimated using digestion solution vials for COD 3–150 mg/L range in conjunction with the digital reactor block DBR 200 and the spectrophotometer DR5000 manufactured by HACH. Concentrations of soluble phosphate (PO_4^{3-}-P), nitrate (NO_3^--N) and nitrite (NO_2^--N) were estimated with a 930 Compact IC Flex Metrohm Ion Chromatograph (IC) and a Metrosep A Supp 4 250/4.0 column at 25 °C. The IC eluent was 1.7 mM $NaHCO_3$ and 1.8 mM Na_2CO_3 per liter of MilliQ water. The suppressant used was 0.5 M of H_2SO_4 injected at a flow rate of 1.0 mL/min and a volume of 20 μL. The concentration of soluble NH_4^+-N was measured using an 883 Basic IC Plus Metrohm Ion Chromatograph with a Metrosep C6 150/4.0 column and a Metrosep A Supp 4 mm diameter guard column. The cation eluent was 1.7 mL 1 N HNO_3 and 284.1 mg of dipicolinic acid per liter of Milli-Q water, with a flow rate of 0.9 mL/min and 20 μL injection volume. High and low range calibration curves were created for all ions and anions of interest and used to estimate the concentrations of the collected samples. Detection limits for anions and ions were 0.1 mg/L.

2.3. Serum bottle tests with nitrite and nitrate as electron acceptors

Serum bottle tests were performed in triplicates including a control. Towards the completion of the anaerobic cycle, 50 mL of mixed sludge was collected from the reactor. The mixed sludge was rinsed three times with DI water. Stock solutions of 1000 mg/L of PO_4^{3-}-P, NO_2^--N, and NO_3^--N were prepared using Na_2HPO_4, $NaNO_2$, and $NaNO_3$ respectively. Each serum bottle had a total volume of 50 mL and, 5 mL of rinsed sludge was added to each serum bottle. A 0.5 mL concentrated PO_4^{3-}-P solution was added to each serum bottle to provide a final concentration of 10 mg P/L. Synthetic wastewater with the similar composition as in the SBR was used in the serum bottle experiments. The pH was adjusted to 7.4 to match the pH in the reactor. During the beginning of the experiment, 5 mL of the homogenized contents were extracted and the TSS and VSS were measured per the protocol detailed in section 2.2. An aquarium pump supplied air during the aerobic stage. For the anoxic tests, NO_2^--N, and NO_3^--N were added individually as the electron acceptor to final concentrations of 10 mg N/L. Anoxic conditions were ensured by purging the serum bottle contents with nitrogen gas prior to the addition of PO_4^{3-}-P and the sludge. Samples were obtained at 0, 10, 20, 30, 60, and 120 min. All the samples were filtered immediately employing a syringe filter with 0.22 μm pore size, PES, 25 mm, manufactured by Thermo Scientific.

2.4. Polyhydroxyalkanoates (PHAs) and glycogen extraction and quantification

The main polyhydroxyalkanoates identified in sludge performing biological phosphorus removal are poly-3-hydroxybutyrate (PHB), polyhydroxy valerate (PHV), poly-beta-hydroxy-2-methyl valerate (PH2MV). To quantify the PH2MV, PHB, PHV, and glycogen, mixed sludge with a total volume of 30 mL were extracted from the reactor at the culmination of the anaerobic and aerobic phase, the settled biomass was rinsed with DI water three times. After further centrifuging the rinsed sludge for 5 min at 10,000 rpm, the supernatant was discarded. The biomass was placed in a 55 mm diameter aluminum tray and dried at 106 °C for 30 min. The sample was placed inside a desiccator and left overnight for final drying. A sample of dried biomass was weighted and placed inside a Pyrex ® culture tube with a screw cap and a PTFE liner, 0.5 mL of concentrated HCl by Fisher Chemical were mixed with the biomass and incubated at 100 °C for 1 h using a digital reactor block DBR 200 manufactured by HACH. After the sample was cooled down, 1.5 mL of n-propanol, anhydrous 99.9% by Alfa Aesar were added and 20 μL of a solution containing 1 mg/mL of benzoic acid $\geq$ 99.9% manufactured by Sigma-Aldrich in n-propanol was used as internal standard. Subsequently, the sample was vortexed and incubated for 1 h at 100 °C. After cooling the sample at ambient temperature, 4 mL of Milli-Q water and 1 mL of hexane (Fisher Chemicals) were added to the sample to enhance phase separation, and the contents of the tube were first vortexed for 10 s followed by centrifugation at 3000 rpm for 2 min. Following phase separation, 4 mL of the underlying aqueous solution was extracted and wasted using a disposable glass Pasteur pipet. A second aliquot of 4 mL of Milli-Q water was employed to rinse the solvent phase of acid and vortexed for 10 s. Removal of solid debris present in the upper solvent phase was accomplished by centrifuging the sample for 5 min at 3000 rpm.

1 μL of the upper solvent phase was extracted with pipette made of glass and transferred to a gas chromatograph vial for analysis. A 7890A GC system (Agilent technologies) furnished with a flame ionization detector (FID) and a FFAP EC-1000 column 15 m in length, 0.530 μm in diameter, and 1.2 μm film, manufactured by Alltech columns was used to quantify the PHAs and glycogen. The column temperature at the beginning of the run was set at 60 °C and held for 2 min at this temperature, subsequently the temperature was increased at 10 °C/min until it arrived to 140 °C, 40 °C/min until it arrived to 220 °C with a 5-minute holding time to ensure the column was cleaned at the culmination of each test. The sample was analyzed using a split less inlet, the column operated with a constant flow rate of 14 mL/min. FID was set at 240 °C with an H_2 flow rate set at 30 mL/min, an air flow rate set at 300 mL/min, and make up the flow with helium at 12 mL/min. Calibration curves were prepared using Poly(3-hydroxybutyric acid-co-3-hydroxyvaleric acid) manufactured by Sigma-Aldrich as standard for PHB and PHV, 2-Hydroxyhexanoic acid 98% manufactured by Sigma-Aldrich was used as PH2MV standard and glucose was used as a standard to quantify glycogen as glucose. At the conclusion of the anaerobic, aerobic, and anoxic phases, samples were collected and investigated for PHAs and glycogen content.

2.5. mRNA extraction for gene expressions

Biomass was harvested from 1 mL of mixed liquor by centrifugation at 7,000 g for 30 s immediately after collecting from the reactor. After wasting the supernatant, and adding 800 μL of the RNA lysis buffer, the solution was mixed by pipetting. The slurry was pipetted to a Lysis Matrix E (MP Biomedicals, USA) tube before bead beating employing a BEAD RUPTOR 12, manufactured by Omni-International, USA. The bead beating was set to run for 3 cycles at 6 m/s operating for one minute and idling for five minutes in between. The lysates were then kept at 4 °C for

total RNA extraction the following day using Quick-RNA Kits manufactured by Zymo Research, USA. The digestion of the genomic DNA (gDNA) was performed in two rounds. First with the on-column DNase provided in the kit and followed by TURBO^{TM} DNase manufactured by ThermoFisher, USA and digested following the procedure supplied by ThermoFisher, USA. Quality verification and concentration measurements of the gDNA-depleted RNA were performed using a NanoDrop 2000c unit manufactured by ThermoFisher, USA.

2.6. Functional gene expression and cycle analysis

Complete gene expression was performed for each phase using reverse-transcript quantitative PCR (RT-qPCR). Biomass corresponding to the cycle analysis was collected from the reactor and stored in RNAlater (Sigma Aldrich, USA) and processed the next day. qPCR was performed on QuantStudio3 (ThermoFisher, USA) to quantify Accumulibacter's 16S rRNA, *ppk1-IA, and phaC*, denitrifying genes *narG*, *nirS, and, nirK*, and the reference gene *rpoN* or RNA polymerase sigma-54 factor (σ54). The qPCR normalization of *Accumulibacter*, was performed as detailed by other researchers in the past, using *rpoN*, as a constitutive gene (Hong., et al 2023). The *Accumulibacter and* ammonium oxidizing bacteria specific primers and PCR conditions were adopted from He et al., (2007) and Rotthauwe et al., (1997) respectively. Due it its high abundance, the cDNA samples of *Accumulibacter's* 16S rRNA were diluted using a dilution factor of 100 prior to performing qPCR amplification. SYBR green chemistry was employed to perform the qPCR analysis. The total volume of each qPCR reaction was 20 μL which included 10 μL of PowerUp SYBR Green master mix manufactured by ThermoFisher, USA, 6 μL of nuclease-free water, 1 μL of each primer (forward and reverse) and 2 μL of template. Gene expression was estimated using the comparative threshold cycle C_T identified as the $\Delta\Delta C_T$ method Schmittgen and Livak (2008).

2.7. qPCR analysis and conditions

A real-time PCR system, QuantStudio 3 manufactured by Thermo Fisher Scientific was employed to perform qPCR and to calculate the absolute abundance of key functional genes. The samples were mixed manually and prior to performing the qPCR, the well plates were placed in a microplate centrifuged and run for 60 s. The PCR volume and conditions were those explained in Hong et al., (2023). The biomarkers for different functional genes were taken from (Throbäck et al., 2004, Henry et al., 2004 and Caporaso et al., 2011). To perform the absolute quantification of the functional genes, a five-point calibration curve with known standards was generated by 10-fold serial dilution with triplicates for each assay ranging from 10^3 to 10^7 target copies for each reaction, with negative controls run on each plate. The absolute abundance of *nirK*, *nirS* and *ppk1* genes were estimated by using DNA standard as absolute quantification standard. The 16S (515f_806r) rRNA genes were quantified from DNA samples gathered at the beginning and at the culmination of each cycle and run in duplicates. The mean of each sample was used to estimate the average gene number for the 16S rRNA and was used as the DNA standard. Finally, the absolute quantification of each gene was estimated by normalizing the samples with the DNA standard and normalized to the samples taken at $t = 0$.

2.8. DNA extraction and microbial analysis through 16S rRNA sequencing

Sludge from the batch reactor was collected and genomic DNA (gDNA) was extracted from the samples as detailed earlier (Hong et al., 2023). The concentrations of DNA were estimated employing a spectrophotometer Nanodrop 1000 manufactured by Nanodrop technologies, USA. After extraction, all DNA samples were stored at −20 °C. To process, the DNA samples were diluted to 20 ng/μL and sent to Genomics Core, research technology support facility (RTSF) located at Michigan State University for microbial community analysis. The analysis included the amplification of the hypervariable region between V4 and V5 of the 16S rRNA gene. Assignment of taxonomy was performed by using QIIME 2 pipeline version 2019.10 (Bolyen et al., 2019). Taxonomic classification was performed running the SILVA database. Quality control of the data was performed employing the software package Divisive Amplicon Denoising Algorithm (DADA2).

3. Results and discussion

3.1. Performance of reactor during COD removal

The average COD in the influent to the reactor was 424.82 ± 91.22 mg/L (Fig. 1A). The average COD in the reactor effluent was 17.33 ± 12.67 mg/L throughout phase I. During all the subsequent phases, nearly all the COD was consumed by the bacteria present in the reactor as shown in Fig. 1A. Overall, all the readily biodegradable COD represented by the mixture of different VFAs was consumed during the anaerobic phase within the first 15 to 30 min depending upon the type of VFAs present in the influent (based on complete cycle analyses, see section 3.4). Occasional spikes in COD during the aerobic phase were recorded, perhaps due to the release of carbon stored intracellularly during the anaerobic phase by microorganisms present in the reactor.

3.2. Phosphorus removal in the reactor

Phase I. The average PO_4^{3-}-P influent concentration in the reactor was 9.38 ± 0.61 mg/L. Fig. 1B, shows the overall reactor performance and P removal percentages during all phases. During the first 67 days into phase I, the reactor achieved an average PO_4^{3-}-P removal of 87.26 ± 4%. On day 67, the reactor pH was adjusted from 6.9 to 7.5 to 7.4–7.8 range resulting in an average PO_4^{3-}-P removal efficiency greater than 98 % with PO_4^{3-}-P in the final effluent often below detection limits, indicating the higher pH contributed to improved reactor performance. Operational issues with pH probes and acid/base pumps impacted the performance of the reactor at a couple of occasions and when the pH fell below 6.5, PO_4^{3-}-P and NH_4^+-N removal deteriorated. Low pH has been shown to inhibit the growth of PAOs and inactivate the acetate metabolism (Freitas et al., 2009). Alkalinity in the reactor was increased on day 90 to 830 mg/L of $NaHCO_3$ or 498 mg/L of alkalinity as $CaCO_3$. The higher alkalinity, increased nitrification rate in the reactor as shown in Fig. 1C. An increase in alkalinity has been linked to improved phosphorus removal, and enhanced growth and carbon storage by PAOs also (Yang et al., 2020).

Phase II and onwards. Phosphorus removal in the reactor in phase II remained stable with effluent concentrations mainly non-detectable. The occasionally elevated concentrations of PO_4^{3-}-P in the effluent were connected to pH upsets related to issues with the pH probe or acid/base pump issues. During phases III and IV, the PO_4^{3-}-P concentrations in the effluent were below detection limits consistent with the previous phase.

Overall, the data shows that the use of different ratios and types of VFAs did not seem to have a distinguishable effect on the overall phosphorus removal in the reactor from an engineering standpoint. The variability of VFAs did not appear to affect the PO_4^{3-}-P release and uptake by the PAOs. The experimental PO_4^{3-}-P release and uptake rates of the reactor for all four phases are displayed in Table 2. The highest P-release rate was observed in phase II and was estimated to be 0.0329 mg P/mg VSS h, in contrast the lowest aerobic P-uptake rate occurred during phase II and was estimated to be 0.0080 mg P/mg VSS h. The highest P-uptake rates corresponded to phases I and IV which are the phases with highest molecular weight carbon sources.

3.3. Reactor performance regarding nitrogen removal

The average NH_4^+-N influent concentration in the reactor was 25.46

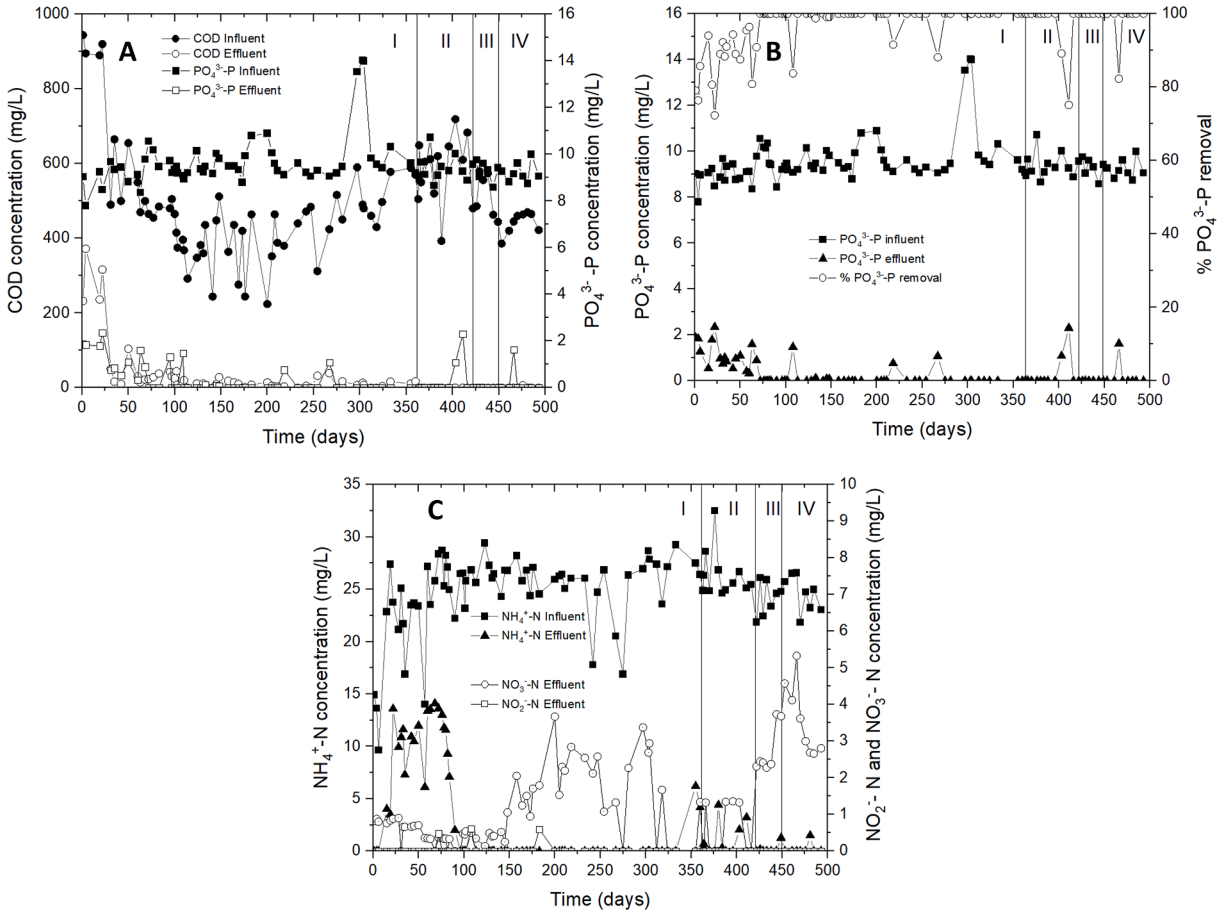

Fig. 1. **A.** COD and phosphorus removal reactor performance. **B.** Phosphorus removal reactor performance. **C.** Nitrogen removal reactor performance.

Table 2
Specific P release and uptake rates calculated from the BNR reactor during a cycle analysis.

Description	Phase I	Phase II	Phase III	Phase IV
Anaerobic P-release rate (mg P/mg VSS h)	0.0324	0.0329	0.0226	0.0299
Aerobic P-uptake rate (mg P/mg VSS)	0.0162	0.0080	0.0103	0.0121

± 3.9 mg/L (Fig. 1C). During the first 89 days of operation, the reactor achieved an average NH_4^+-N removal of 63.56 ± 4.1%, after the alkalinity in the reactor was increased from 12 mg/L of $NaHCO_3$ per mg/L of NH_4^+-N to 32.6 mg/L of $NaHCO_3$ per mg/L of NH_4^+-N or approximately 498 mg/L of alkalinity as $CaCO_3$, the average NH_4^+-N removal in the reactor increased to 96.73 ± 2.5%. Nitrification is inhibited under low alkalinity conditions. The results obtained in this investigation are in alignment with recent experiments showing that increased alkalinity enhances NH_4^+-N removal (Gao et al., 2020). The total inorganic nitrogen TIN removal of 98.62% was achieved at an alkalinity of 500 mg/L as $CaCO_3$ by Gao et al., 2020. During phase I, and after the alkalinity was increased to 478 mg/L as $CaCO_3$, the nitrification process became stable and consistent. During phase II, a decrease in the nitrification rate was observed, possibly due to pH upsets. Throughout phases III and IV, the nitrification performance of the reactor continued to be stable. There was no NO_2^--N accumulation in all four phases, showing that the reactor performed complete nitrification. NO_3^-N was measured in the effluent during all four phases, indicating incomplete denitrification during the anoxic phase, possibly due to carbon limitation (see COD in Fig. 1A). There were several instances where complete denitrification was achieved in phases I and II, interestingly, the PHAs produced during phase I and II were the highest among all four phases. This finding proposes that increased production of PHAs can lead to improved denitrification due to the capacity of bacteria to use the internally stored polymer for denitrification purposes.

3.4. Full cycle analyses to track the fate of different contaminants during a complete cycle

Cycle analysis for the fate of P and COD during a complete cycle were performed during all four phases and the results were shown in Fig. 2A–D. During phases I and IV that contained feed with higher molecular weight VFAs, it was observed that the soluble COD in the bulk liquid took longer time to reach below detection limits than in phases II and III that contained lower molecular weight VFAs where the soluble COD was completely consumed by the bacteria within the first 15 min of supplying the carbon.

Full cycle analysis as shown in Fig. 2B for phase II, revealed that approximately 93.5 ± 2.2% of the PO_4^{3-}-P released in the reactor occurred through the initial 15 min of the anaerobic cycle with 84 ± 3.1% consumption of the readily available COD. After approximately 45 min, no more PO_4^{3-}-P release took place, coinciding with no significant decrease in the available COD. The use of a mixture of VFAs as a carbon source under the given conditions appears to accelerate the release of phosphorus by providing the microorganisms with readily available COD. Readily available COD such as short chain VFAs can be utilized as a source of carbon during denitrification (Jiang et al., 2013) and phosphorus removal (Abu-Ghararah et al., 1991).

The specific PO_4^{3-}-P uptake and release rates in the reactor are shown in Table 2, the VSS used for the calculation was the average of samples

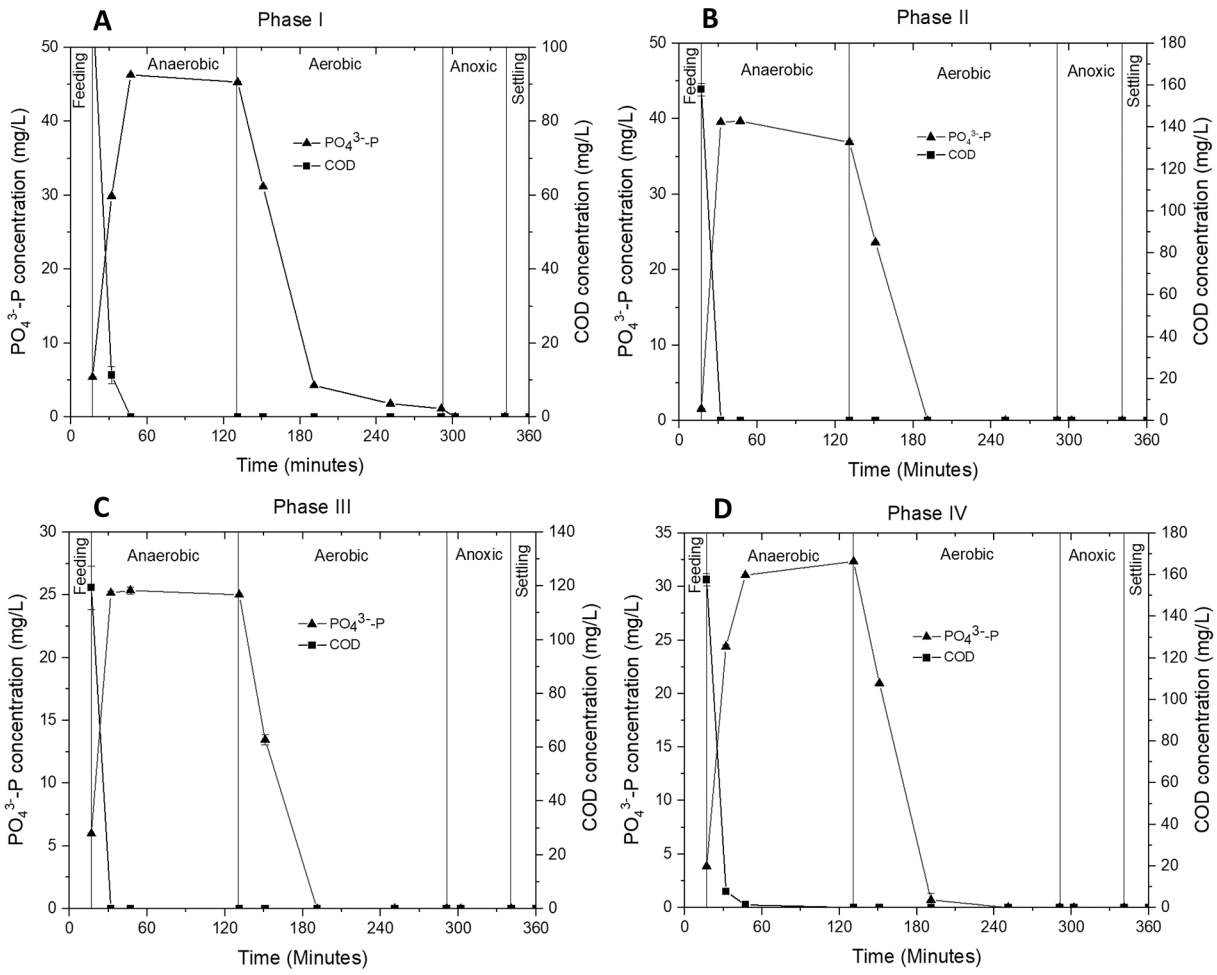

Fig. 2. **A.** Complete cycle alalysis: Phosphorus and COD removal during phase I. **B.** Phosphorus and COD removal during phase II. **C.** Phosphorus and COD removal during phase III. **D.** Phosphorus and COD removal during phase IV.

taken at the start and at the end of the cycle. Phosphorus uptake during anoxic conditions was observed, although the P-uptake was several orders of magnitude lower than that during aerobic conditions. The decrease in PO_4^{3-}-P corresponded with a reduction in NO_3^--N concentrations which points toward the potential presence of DPAOs. The serum bottle data presented later in this manuscript supports this notion about the potential role of DPAOs towards anoxic-P uptake.

The complete cycle analysis results for nitrogen species are presented in Fig. 3A–D. Complete nitrification and denitrification were observed during the sampling day during phase I. During phase I, which corresponds to the occurrence of higher molecular weight acids in the feed, the nitrification and denitrification process were completed during the aerobic and anoxic cycle respectively. Key functional genes were expressed and their expression was analyzed to determine the reactions of the microbial populations to the dynamics of the chemical species during the cycle. All RNA samples had 260/280 and 230/260 values of at least 2, suggesting their high quality. qPCR was run for *Accumulibacter* 16S rRNA (without reverse transcription) and the average difference in C_T value among the RNA and the cDNA samples of the gene was about 20 cycles, indicating minimal gDNA contaminations.

Fig. 4A gene expression of *Accumulibacter* and AOBs across the cycle. *ppk1* gene from *Accumulibacter* is known as responsible for the synthesis of polyphosphate. The *phaC* gene from *Accumulibacter* is known to be responsible for the biosynthesis of PHA. The expression of *ppk1-IA* increased at the beginning of the anaerobic and aerobic phases, where the majority of P-release and P-uptake took place, respectively. Nevertheless, the expression of *phaC* was muted in the anaerobic phase despite PHA being accumulated. Previous studies also reported similar findings He and McMahon (2011). In the aerobic phase, *phaC* expression increased gradually throughout and at the beginning of the anoxic phase. The patterns suggest that the upregulation of *phaC* occurred when there was a need for intracellular PHA usage, in this case, for the P-uptake and denitrification, which took place in the aerobic and anoxic phases, respectively. The expression patterns of the *Accumulibacter* 16S rRNA gene showed a relatively constant pattern in the anaerobic phase while rising in the aerobic phase similar to an earlier study (Hong et al., 2023). These findings suggest that *Accumulibacter* were preparing for growth by increasing the production of their rRNA during the aerobic phase agreeing with the EBPR metabolic models (He and McMahon, 2011;Otto et al., 2019). As expected, the expression of *amoA* increased in the aerobic phase while NH_4^+-N was removed. In the anaerobic phase, the expression of the genes *nirS* and *nirK* responsible for nitrite reductase and nitrate reductase (*narG*) increased (Fig. 4B). The increase was due to NO_x^--N carry-over from the previous cycle, making the beginning of the cycle anoxic rather than truly anaerobic. The expression of the genes decreased sharply in the aerobic phase while increasing the anoxic phase. The targeted *Candidatus* Accumulibacter clades were IIA, IIB, IIC and IID. During Phase I, only Acc-ppk1-254f-460r primer amplified, which corresponds to clade IIC. The PCR efficiencies ranged between 98% and 106% with an R^2 of 0.986, showing the accuracy of the qPCR assay.

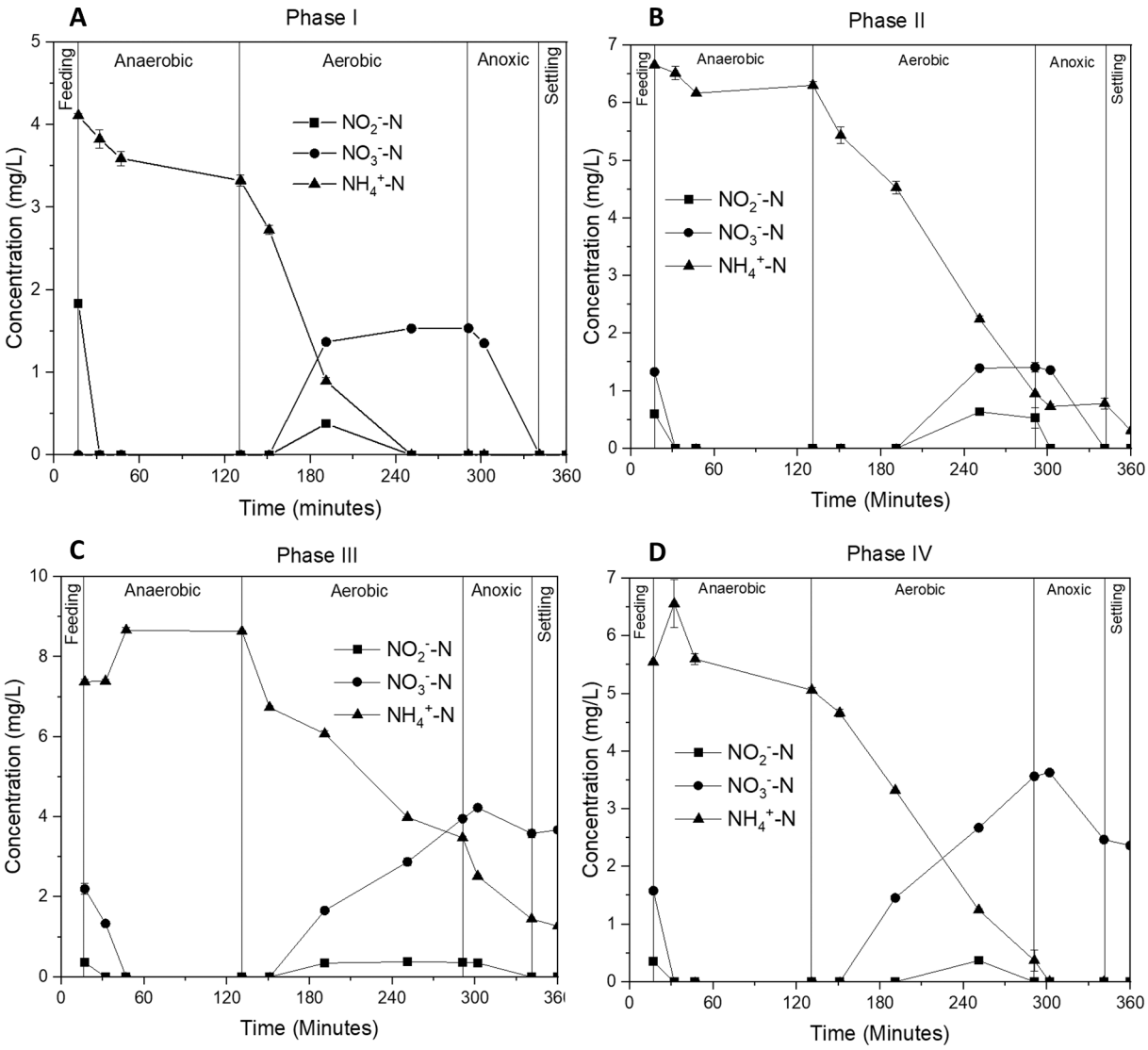

Fig. 3. A. Complete cycle analysis: Nitrification and denitrification during Phase I. **B.** Nitrification and denitrification during Phase II. **C.** Nitrification and denitrification during Phase III. **D.** Nitrification and denitrification during Phase IV.

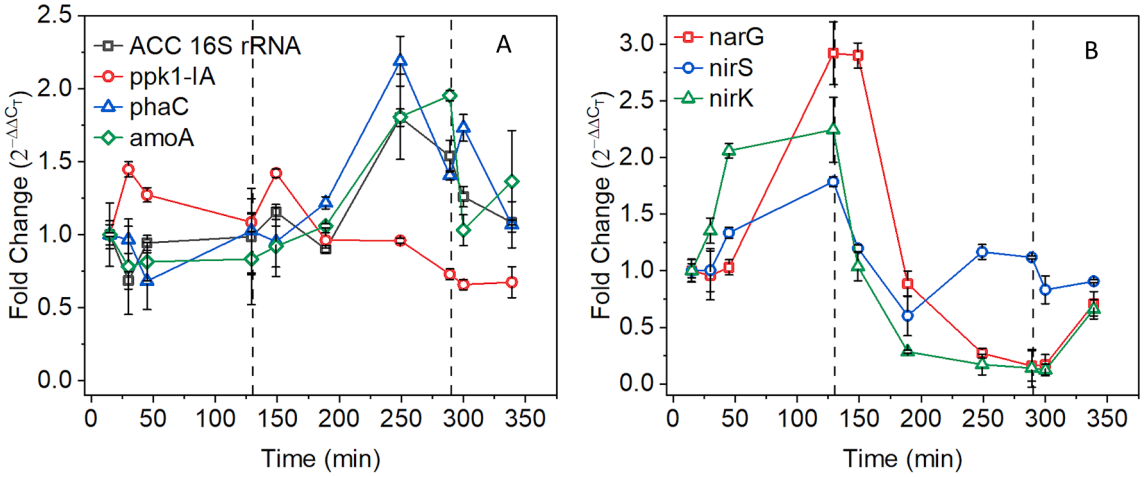

Fig. 4. Gene expression profile during a cycle. **A.** Expression profile of Accumulibacter's 16S rRNA gene, *ppkl-IA*, *phaC*, and *amoA*. **B.** expression profile of denitrifying genes *narG*, *nirsS*, and *nirK*.

3.5. Specific phosphorus uptake during aerobic and anoxic conditions

Serum bottle tests were done to determine the aerobic and anoxic phosphorus uptake rates. The anoxic phosphorus uptake tests were done to estimate the possible role of DPAOs. Serum bottle tests using the sludge from the reactor, indicate the presence of PAOs and DPAOs capable of using O_2 and NO_2^--N as electron acceptors for P uptake respectively. When NO_3^--N was used, no P uptake was recorded. On the contrary, P release was detected with nitrate present indicating secondary P release. Tests plots for data for experiments conducted with different electron acceptors are available in Supplementary Fig. S1A–C. The serum bottles tests show that O_2 was a more efficient electron acceptor than NO_2^--N with a much faster P-uptake. The results showed that when O_2 was used as electron acceptor, complete P-uptake was achieved within 30 min, contrary to using NO_2^--N, that after 120 min, the P concentration was still around 0.8 mg/L, an indication that longer anoxic cycle time will be required for complete P-uptake. The specific P uptake rates and the NO_2^--N consumption rates during the serum bottles tests are displayed in Table 3. The highest rate for P-uptake under aerobic conditions was achieved in phase IV with a 0.0219 ± 0.0041 mg P/mg VSS h. The serum bottles tests indicated the presence of DPAOs, with the ability to use NO_2^--N as electron acceptor for phosphorus uptake under anoxic conditions. DPAOs with the capacity to perform denitrification and P-uptake simultaneously can represent significant carbon savings for WWTPs and will benefit plants with weak wastewater influents.

3.6. Polyhydroxyalkanoates (PHAs) formation and utilization analysis

During all phases, acetate and propionate were mainly used for the production of PH2MV and PHB with smaller production of PHV. During phase I, total PHAs towards the end of the anaerobic phase averaged 1.36% of dried biomass with PHAs decreasing by an average of 79% to 0.00274 ± 0.00106 mg PHAs/mg of dry biomass towards the end of the aerobic phase. During phase II, at the culmination of the anaerobic phase, the total PHAs represented an average of 1.62% of dried biomass. In phase II of the experiment, where acetic acid composed the majority of the VFAs fed to the reactor, PHB was the top PHA produced. This finding coincides with Pijuan et al., 2004 that found acetate mostly stored in the form of PHB. During phase III, at the culmination of the anaerobic phase, the total PHAs represented an average of 1.12% of dried biomass. Under anaerobic conditions, VFAs were converted to PHAs and the P release occurred. During aerobic conditions, PHAs were used for cell growth, and P uptake took place. During anoxic conditions while denitrification took place, depletion of all identified PHAs (PHB, PHV, and PH2MV) was detected. Lack of carbon sources during denitrification can lead to the carbon limitation for denitrification to occur efficiently (Krasnits et al., 2013). Partial denitrification during phases III and IV and complete denitrification during phases I and II, without the requirement to add external carbon sources during the anoxic stage were recorded.

During phase IV, at the conclusion of the anaerobic phase, the total PHAs represented an average of 0.93% of dried biomass. A summary of all the quantified PHAs obtained at the culmination of each cycle and at each phase is shown in Table 4. PH2MV was the number one polymer present in the biomass during phases I and III, followed by PHB and PHV. During phase II, with acetic acid as the principal carbon source, the main stored polymer was PHB, consistent with results obtained by Kedia et al., 2014.

During phases I and III, where the percentages of acetic and propionic acid present in the influent VFAs were almost the same, PH2MV was mainly produced followed by PHB. The metabolic pathway for propionic acid used by PAOs consists of the assimilation of propionic acid by PAOs and its transformation to propionyl-CoA by hydrolyzing the accumulated Poly-P and glycogen and using them as a source of energy. The metabolic pathway for acetic acid used by PAOs consists of the uptake of acetic acid by PAOs and its transformation to acetyl-CoA by hydrolyzing the stored Poly-P and glycogen and using them as a source of energy. Understanding the metabolic pathways used by microorganisms, is important from an engineering point because it can allow to improve the performance of the bacterial strains in the generation of PHAs. The polymer PHV consistently accounted for the lowest concentration in all four phases, the production of this polymer was possibly through the modified succinate-propionate pathway or the TCA cycle. The highest PHA formation during the anaerobic phase was obtained in phase II with 0.01618 ± 0.00202 mg/mg of dry biomass. Hollender et al., 2002, estimated PHA storage during anaerobic cycle to be 20 mg C/g of dry matter while using acetate as the only source of carbon. Overall, the formation of PHAs occurred at the culmination of the anaerobic cycle with phase II providing the highest amount of PHAs of 0.01618 ± 0.00202 mg PHA/mg of dry biomass. The highest consumption rate of PHAs occurred during the aerobic cycle with smaller consumption observed during the anoxic cycle.

3.7. Glycogen formation and utilization analysis

Regeneration of glycogen was detected at the culmination of the aerobic cycle during all four phases and depletion of glycogen was observed in all phases at the end of anaerobic cycles as observed in Fig. 5A–D. These results are aligned with observations by other researchers (Acevedo et al., 2012) where PHAs were employed as energy and carbon sources during the aerobic and anoxic phases to replenish glycogen and store poly-P. The concentrations of glycogen extracted from the dry biomass during all phases were consistently higher by a factor of 9 ± 1 with glycogen being depleted during the anaerobic cycle by approximately 10%. The highest glycogen storage at the end of the aerobic cycle was achieved in phase I with 0.17221 ± 0.02157 mg glycogen as glucose/mg of dry biomass. The estimated value was significantly higher than the 17 mg C/g of dry matter obtained at the conclusion of the aerobic cycle on a reactor fed with acetate by other researchers (Hollender et al., 2002).

3.8. Microbial community analysis

Throughout the reactor operation, the phylum with the highest relative abundance was Proteobacteria, followed by Bacteroidetes, see Fig. 6A. Phyla Chloroflexi was also found but at a lower relative abundance in all four phases. Phylum Proteobacteria, Bacteroidetes, and Chloroflexi have been found in major relative abundance in dissolved-P removal biological processes suggesting that they have a key part in nutrient removal (Li et al., 2020). The Proteobacteria phyla have been identified as prevalent in nutrient removal processes (Liu et al., 2016) and play a significant role in biological nutrient removal and nutrient cycling (Wang et al., 2020). The phyla Chloroflexi comprises facultative microorganisms with diverse metabolic pathways (Santos et al, 2020), some with the capacity to act as a nitrite oxidizer (Zhao et al., 2012). At the genus level, the two genera with the utmost relative abundance were *Candidatus* Accumulibacter and *Defluviicoccus*, which suggests that these two genera have an essential function in BNR processes, see Fig. 6B. *Candidatus* Accumulibacter is considered a polyphosphate-accumulating organism (Kolakovic et al., 2021) with high relative abundance in

Table 3
Calculated specific P uptake and N use rates from serum bottles test.

Description	Phase I	Phase II	Phase III	Phase IV
Aerobic P-uptake (mg P/mg VSS h)	0.0094 ± 0.00096	0.0092 ± 0.00025	0.0093 ± 0.00082	0.0219 ± 0.0041
Anoxic P-uptake (NO_2) (mg P/mg VSS h)	0.0107 ± 0.00091	0.0036 ± 0.00129	0.0028 ± 0.00150	0.0048 ± 0.0020
Anoxic NO_2 use (mg N/mg VSS h)	0.0092 ± 0.00113	0.0027 ± 0.00162	0.0029 ± 0.00190	0.004 ± 0.0026

Table 4
PHAs measured at the end of the anaerobic and aerobic cycles during the four phases.

Phase	Anaerobic			Aerobic		
	PHB (mg/mg of dry biomass)	PHV (mg/mg of dry biomass)	PH2MV (mg/mg of dry biomass)	PHB (mg/mg of dry biomass)	PHV (mg/mg of dry biomass)	PH2MV (mg/mg of dry biomass)
I	0.00435 ± 0.000820	0.00346 ± 0.00059	0.00580 ± 0.00101	0.00087 ± 0.00026	0.00064 ± 0.00249	0.00123 ± 0.00055
II	0.00666 ± 0.000570	0.00369 ± 0.00043	0.00583 ± 0.00119	0.00183 ± 0.00054	0.00091 ± 0.00026	0.00204 ± 0.00024
III	0.00340 ± 0.000190	0.00245 ± 0.00020	0.00539 ± 0.00043	0.00087 ± 0.00036	0.00050 ± 0.00020	0.00133 ± 0.00063
IV	0.00382 ± 0.001140	0.00358 ± 0.00102	0.00504 ± 0.00157	0.00161 ± 0.00037	0.00139 ± 0.00028	0.00201 ± 0.00057

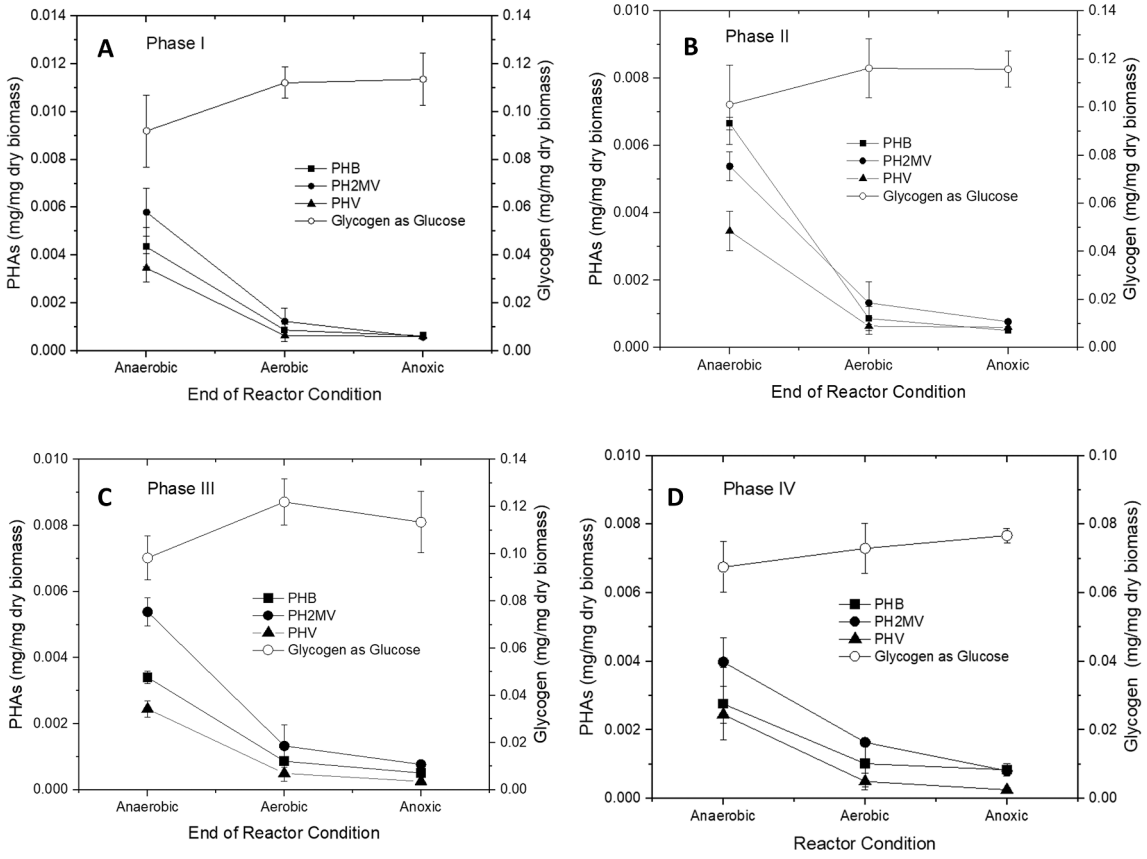

Fig. 5. PHAs and glycogen concentrations **A.** Phase **B.** Phase II **C.** Phase III **D.** Phase IV.

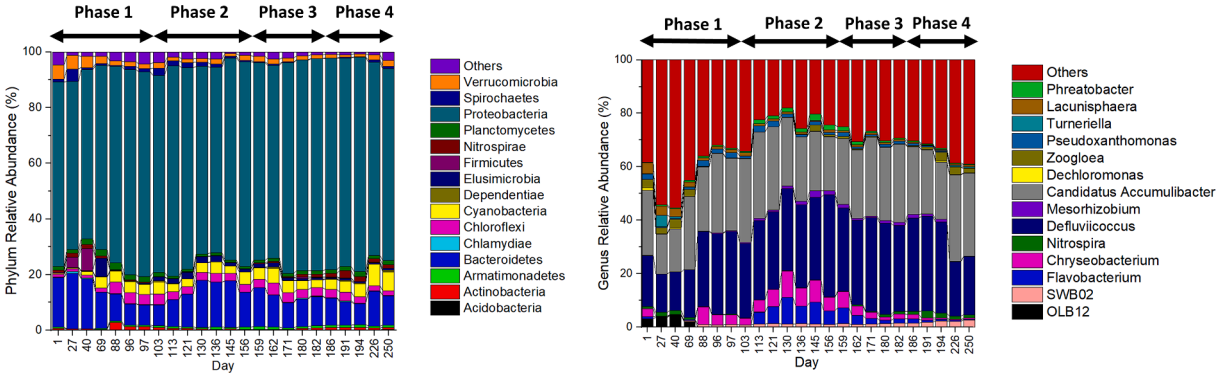

Fig. 6. A. Relative abundance at phylum level, others include no hits, unclassified and unknown data. B. Relative abundance at genus level. Others include all classified genus with less than 0.2% relative abundance, unknown, no hits and unclassified data.

nutrient removal and EBPR processes (Oyserman et al., 2016). The genus *Chryseobacterium* and *Zoogloea*, were also present in the reactor throughout the reactor at a lower relative abundance on all four phases. The reactor had good nutrient removal performance throughout the four phases with a high relative abundance of the genus *Candidatus* Accumulibacter. Good performance and stability of nutrient removal

processes have been connected to the high abundance of *Candidatus* Accumulibacter (Lu et al., 2006, Oehmen et al., 2006). The presence of *Defluviicoccus* in the reactor did not cause a detriment in the performance of nutrient removal and a stable nutrient removal was achieved in the reactor despite that the relative abundance of *Defluviicoccus* was higher than the relative abundance of *Candidatus* Accumulibacter during all four phases. This observation agrees with Mielczarek et al., 2013 that analyzed data from several Danish WWTPs where the presence of *Defluviicoccus* did not translate into poor phosphorus removal. The presence of *Defluviicoccus* was linked to the upset of an EBPR process by Meyer et al., 2006 but our data did not show performance deterioration. *Defluviicoccus* have metabolic pathways that are present in GAO's and could be considered putative GAOs (Wong et al., 2004). *Defluviicoccus* have been identified in many full scale WWTPs that perform nutrient removal (McIlroy et al., 2009). *Defluviicoccus* can anaerobically take carbon sources such as propionate and acetate, indicating carbon competition with PAOs. Some species of Chryseobacterium have shown high sludge reduction capabilities (Wang et al., 2021). The highest relative abundance of the bacterial communities in the reactor shifted at the phylum (Proteobacteria and Bacteroidetes) and genus (*Candidatus* Accumulibacter and *Defluviicoccus*) levels, but overall, *Candidatus* Accumulibacter and *Defluviicoccus* remained as the top two in terms of relative abundances. The analyzed bacterial community provided five different *Nitrosomonas* species and three different *Nitrospira* species. These genera have been associated with nitrification. During phase I, the genus OLB12 was detected in the BNR reactor with relative abundance as high as 4.4% but was not present during the other three phases. The presence of OLB12 in BNR reactors has been linked with phosphorus removal, nitrification processes, and denitrification processes (Li et al., 2022). During phase III, when only acetic and propionic acids were available as carbon sources, it was observed that the genus *Defluviicoccus* had a relative abundance consistently higher than the relative abundance of the genus *Candidatus* Accumulibacter. The dominance of the genus *Defluviicoccus* was also observed by Dai et al., 2007 that identified propionate allowed *Defluviicoccus* maximize the storage of energy and carbon sources, providing them with an advantage over PAOs. Dai et al., 2007, also determined the propionate utilization is enhanced when acetate is present, which was the case for the carbon source provided during phase III of this experiment. During phases I, II, and IV when the reactor was fed with at least three different types of volatile fatty acids, the relative abundance of *Defluviicoccus* and *Candidatus* Accumulibacter shifted back and forth. The results show that *Defluviicoccus* genus has a high affinity for propionic acid, and high amounts of propionic acid enhanced their bacterial dominance.

4. Conclusions

High relative abundance of *Defluviicoccus* did not affect the performance of the BNR process. PHAs were stored mostly in the form of PH2MV when approximately equal percentages of acetic and propionic acid were fed to the reactor, indicating preference for the bacteria community present in this reactor to use the propionic acid metabolic pathway. A combination of VFAs that include higher molecular weight acids like the ratio used during Phase IV, seem to benefit denitrification. DPAO belonging to Clade IIC was detected in the reactor and displayed capability to use NO_2^--N as electron acceptor during phosphorus uptake.

Declaration of Competing Interest

The authors declare that they have no known competing financial interests or personal relationships that could have appeared to influence the work reported in this paper.

Data availability

Data will be made available on request.

Acknowledgments

Ruby Diaz thanks the NDSEG Fellowship program for their financial support to develop this research project. The reactor set-up and other necessary supplies were funded under the NSF Grant # 1804158. The discussion solely presents author's view point and not necessarily reflect on the funding agencies.

Appendix A. Supplementary data

Supplementary data to this article can be found online at https://doi.org/10.1016/j.biortech.2023.129675.

References

Abu-Ghararah, Z.H., Randall, C.W., 1991. The effect of organic compounds on biological phosphorus removal. Water Sci. Technol. 23 (4–6), 585–594.
Acevedo, B., Oehmen, A., Carvalho, G., Seco, A., Borrás, L., Barat, R., 2012. Metabolic shift of polyphosphate-accumulating organisms with different levels of polyphosphate storage. Water Res. 46 (6), 1889–1900.
Bolyen, E., Rideout, J.R., Dillon, M.R., Bokulich, N.A., Abnet, C.C., Al-Ghalith, G.A., Alexander, H., Alm, E.J., Arumugam, M., Asnicar, F., Bai, Y., Bisanz, J.E., Bittinger, K., Brejnrod, A., Brislawn, C.J., Brown, C.T., Callahan, B.J., Caraballo-Rodríguez, A.M., Chase, J., Cope, E.K., Da Silva, R., Diener, C., Dorrestein, P.C., Douglas, G.M., Durall, D.M., Duvallet, C., Edwardson, C.F., Ernst, M., Estaki, M., Fouquier, J., Gauglitz, J.M., Gibbons, S.M., Gibson, D.L., Gonzalez, A., Gorlick, K., Guo, J., Hillmann, B., Holmes, S., Holste, H., Huttenhower, C., Huttley, G.A., Janssen, S., Jarmusch, A.K., Jiang, L., Kaehler, B.D., Kang, K.B., Keefe, C.R., Keim, P., Kelley, S.T., Knights, D., Koester, I., Kosciolek, T., Kreps, J., Langille, M.G.I., Lee, J., Ley, R., Liu, Y.-X., Loftfield, E., Lozupone, C., Maher, M., Marotz, C., Martin, B.D., McDonald, D., McIver, L.J., Melnik, A.V., Metcalf, J.L., Morgan, S.C., Morton, J.T., Naimey, A.T., Navas-Molina, J.A., Nothias, L.F., Orchanian, S.B., Pearson, T., Peoples, S.L., Petras, D., Preuss, M.L., Pruesse, E., Rasmussen, L.B., Rivers, A., Robeson, M.S., Rosenthal, P., Segata, N., Shaffer, M., Shiffer, A., Sinha, R., Song, S.J., Spear, J.R., Swafford, A.D., Thompson, L.R., Torres, P.J., Trinh, P., Tripathi, A., Turnbaugh, P.J., Ul-Hasan, S., van der Hooft, J.J.J., Vargas, F., Vázquez-Baeza, Y., Vogtmann, E., von Hippel, M., Walters, W., Wan, Y., Wang, M., Warren, J., Weber, K. C., Williamson, C.H.D., Willis, A.D., Xu, Z.Z., Zaneveld, J.R., Zhang, Y., Zhu, Q., Knight, R., Caporaso, J.G., 2019. Reproducible, interactive, scalable and extensible microbiome data science using QIIME 2. Nat. Biotechnol. 37 (8), 852–857.
Caporaso, J.G., Lauber, C.L., Walters, W.A., Berg-Lyons, D., Lozupone, C.A., Turnbaugh, P.J., Fierer, N., Knight, R., 2011. Global patterns of 16S rRNA diversity at a depth of millions of sequences per sample. Proc. Natl. Acad. Sci. 108 (supplement_1), 4516–4522.
Chen, Y., Ruhyadi, R., Huang, J., Yan, W., Wang, G., Shen, N., Hanggoro, W., 2021. Comprehensive comparison of acidic and alkaline anaerobic fermentations of waste activated sludge. Bioresour. Technol. 323, 124613.
Dai, Y., Yuan, Z., Wang, X., Oehmen, A., Keller, J., 2007. Anaerobic metabolism of Defluviicoccus vanus related glycogen accumulating organisms (GAOs) with acetate and propionate as carbon sources. Water research 41 (9), 1885–1896.
Diaz, R., Goswami, A., Clark, H.C., Michelson, R., Goel, R., 2023. Volatile fatty acid production from primary and secondary sludges to support efficient nutrient management. Chemosphere 336, 138984.
Freitas, F., Temudo, M.F., Carvalho, G., Oehmen, A., Reis, M.A.M., 2009. Robustness of sludge enriched with short SBR cycles for biological nutrient removal. Bioresource Technology (Elsevier Ltd.) 100 (6), 1969–1976.
Gao, S., He, Q., Wang, H., 2020. Research on the aerobic granular sludge under alkalinity in sequencing batch reactors: Removal efficiency, metagenomic and key microbes. Bioresour. Technol. 296, 122280.
Goel, R.K., Noguera, D.R., 2006. Evaluation of sludge yield and phosphorus removal in a Cannibal solids reduction process. J. Environ. Eng. 132 (10), 1331–1337.
He, S., McMahon, K.D., 2011. '*Candidatus* Accumulibacter' gene expression in response to dynamic EBPR conditions. ISME J. 5 (2), 329–340.
Henry, S., Baudoin, E., López-Gutiérrez, J.C., Martin-Laurent, F., Brauman, A., Philippot, L., 2004. Quantification of denitrifying bacteria in soils by *nirK* gene targeted real-time PCR. J. Microbiol. Methods 59 (3), 327–335.
Hollender, J., van der Krol, D., Kornberger, L., Gierden, E., Dott, W., 2002. Effect of different carbon sources on the enhanced biological phosphorus removal in a sequencing batch reactor. World J. Microbiol. Biotechnol. 18 (4), 359–364.
Hong, S., Winkler, M.-K.-H., Wang, Z., Goel, R., 2023. Integration of EBPR with mainstream anammox process to treat real municipal wastewater: process performance and microbiology. Water Res. 233, 119758.
Jiang, J., Zhang, Y., Li, K., Wang, Q., Gong, C., Li, M., 2013. Volatile fatty acids production from food waste: effects of pH, temperature, and organic loading rate. Bioresour. Technol. 143, 525–530.
Kedia, G., Passanha, P., Dinsdale, R.M., Guwy, A.J., Esteves, S.R., 2014. Evaluation of feeding regimes to enhance PHA production using acetic and butyric acids by a pure culture of Cupriavidus necator. Biotechnol. Bioprocess Eng. 19 (6), 989–995.
Kolakovic, S., Freitas, E.B., Reis, M.A.M., Carvalho, G., Oehmen, A., 2021. Accumulibacter diversity at the sub-clade level impacts enhanced biological phosphorus removal performance. Water Res. 199, 117210.

Krasnits, E., Beliavsky, M., Tarre, S., Green, M., 2013. PHA based denitrification: Municipal wastewater vs. acetate. Bioresour. Technol. 132, 28–37.
Li, Y., Dong, R., Guo, J., Wang, L., Zhao, J., 2022. Effects of Mn2+ and humic acid on microbial community structures, functional genes for nitrogen and phosphorus removal, and heavy metal resistance genes in wastewater treatment. J. Environ. Manage. 313, 115028.
Li, X.i., Li, Y., Lv, D., Li, Y., Wu, J., 2020. Nitrogen and phosphorus removal performance and bacterial communities in a multi-stage surface flow constructed wetland treating rural domestic sewage. Sci. Total Environ. 709, 136235.
Li, X., Peng, Y., Zhao, Y., Zhang, L., Han, B., 2017. Volatile fatty acid accumulation by alkaline control strategy in anaerobic fermentation of primary sludge. Environ. Eng. Sci. 34 (10), 703–710.
Liu, Y., Su, X., Lu, L., Ding, L., Shen, C., 2016. A novel approach to enhance biological nutrient removal using a culture supernatant from Micrococcus luteus containing resuscitation-promoting factor (Rpf) in SBR process. Environ. Sci. Pollut. Res. 23 (5), 4498–4508.
Lu, H., Oehmen, A., Virdis, B., Keller, J., Yuan, Z., 2006. Obtaining highly enriched cultures of *Candidatus* Accumulibacter phosphates through alternating carbon sources. Water Res. 40 (20), 3838–3848.
Luo, J., Huang, W., Zhang, Q., Guo, W., Wu, Y., Feng, Q., Fang, F., Cao, J., Su, Y., 2020. Effects of different hypochlorite types on the waste-activated sludge fermentation from the perspectives of volatile fatty acids production, microbial community and activity, and characteristics of fermented sludge. Bioresour. Technol. 307, 123227.
McIlroy, S., Seviour, R.J., 2009. Elucidating further phylogenetic diversity among the Defluviicoccus-related glycogen-accumulating organisms in activated sludge. Environ. Microbiol. Rep. 1 (6), 563–568.
Meyer, R.L., Saunders, A.M., Blackall, L.L., 2006. Putative glycogen-accumulating organisms belonging to the Alphaproteobacteria identified through rRNA-based stable isotope probing. Microbiology 152 (2), 419–429.
Mielczarek, A.T., Nguyen, H.T.T., Nielsen, J.L., Nielsen, P.H., 2013. Population dynamics of bacteria involved in enhanced biological phosphorus removal in Danish wastewater treatment plants. Water Res. 47 (4), 1529–1544.
Oehmen, A., Saunders, A.M., Vives, M.T., Yuan, Z., Keller, J., 2006. Competition between polyphosphate and glycogen accumulating organisms in enhanced biological phosphorus removal systems with acetate and propionate as carbon sources. J. Biotechnol. 123 (1), 22–32.
Okada, M., Lin, C.K., Katayama, Y., Murakami, A., 1992. Stability of phosphorus removal and population of bio-P-bacteria under short term disturbances in sequencing batch reactor activated sludge process. Water Sci. Technol. 26 (3–4), 483–491.
Otto, M., Wynands, B., Drepper, T., Jaeger, K.E., Thies, S., Loeschcke, A., Blank, L.M., Wierckx, N., 2019. Targeting 16S rDNA for stable recombinant gene expression in Pseudomonas. ACS Synth. Biol. 8 (8), 1901–1912.
Owusu-Agyeman, I., Plaza, E., Cetecioglu, Z., 2020. Production of volatile fatty acids through co-digestion of sewage sludge and external organic waste: effect of substrate proportions and long-term operation. Waste Manag. 112, 30–39.
Oyserman, B.O., Noguera, D.R., del Rio, T.G., Tringe, S.G., McMahon, K.D., 2016. Metatranscriptomic insights on gene expression and regulatory controls in *Candidatus* Accumulibacter phosphatis. ISME J. 10 (4), 810–822.
Pijuan, M., Baeza, J.A., Casas, C., Lafuente, J., 2004. Response of an EBPR population developed in an SBR with propionate to different carbon sources. Water Sci. Technol. 50 (10), 131–138.
Rotthauwe, J.H., Witzel, K.P., Liesack, W., 1997. The ammonia monooxygenase structural gene amoA as a functional marker: molecular fine-scale analysis of natural ammonia-oxidizing populations. Appl. Environ. Microbiol. 63 (12), 4704–4712.
Rout, P.R., Shahid, M.K., Dash, R.R., Bhunia, P., Liu, D., Varjani, S., Zhang, T.C., Surampalli, R.Y., 2021. Nutrient removal from domestic wastewater: A comprehensive review on conventional and advanced technologies. J. Environ. Manage. 296, 113246.
Santos, A., Rachid, C., Pacheco, A.B., Magalhães, V., 2020. Biotic and abiotic factors affect microcystin-LR concentrations in water/sediment interface. Microbiol. Res. 236, 126452.
Schmittgen, T.D., Livak, K.J., 2008. Analyzing real-time PCR data by the comparative CT method. Nat. Protoc. 3 (6), 1101–1108.
Tan, R., Miyanaga, K., Uy, D., Tanji, Y., 2012. Effect of heat-alkaline treatment as a pretreatment method on volatile fatty acid production and protein degradation in excess sludge, pure proteins and pure cultures. Bioresour. Technol. 118, 390–398.
Throbäck, I.N., Enwall, K., Jarvis, Å., Hallin, S., 2004. Reassessing PCR primers targeting *nirS*, *nirK* and *nosZ* genes for community surveys of denitrifying bacteria with DGGE. FEMS Microbiol. Ecol. 49 (3), 401–417.
Vidal-Antich, C., Perez-Esteban, N., Astals, S., Peces, M., Mata-Alvarez, J., Dosta, J., 2021. Assessing the potential of waste activated sludge and food waste co-fermentation for carboxylic acids production. Sci. Total Environ. 757, 143763.
Wang, N.a., Chen, X., Ji, Y., Yan, W., Chui, C., Liu, L.i., Shi, J., 2021. Enhanced sludge reduction during swine wastewater treatment by the dominant sludge-degrading strains Chryseobacterium sp. B4 and Serratia sp. H1. Bioresour. Technol. 330, 124983.
Wang, S., Cui, Y., Li, A., Zhang, W., Wang, D., Chen, Z., Liang, J., 2020. Deciphering of organic matter and nutrient removal and bacterial community in three sludge treatment wetlands under different operating conditions. J. Environ. Manage. 260, 110159.
Wong, M.T., Tan, F.M., Ng, W.J., Liu, W.T., 2004. Identification and occurrence of tetrad-forming Alphaproteobacteria in anaerobic–aerobic activated sludge processes. Microbiology 150 (11), 3741–3748.
Yang, J., Li, Z., Lu, L., Fang, F., Guo, J., Ma, H., 2020. Model-based evaluation of algal-bacterial systems for sewage treatment. J. Water Process Eng. 38, 101568.
Zeng, W., Zhang, J., Wang, A., Peng, Y., 2016. Denitrifying phosphorus removal from municipal wastewater and dynamics of "Candidatus Accumulibacter" and denitrifying bacteria based on genes of ppk1, *narG*, *nirS* and *nirK*. Bioresour. Technol. 207, 322–331.
Zhao, D., Huang, R., Zeng, J., Yan, W., Wang, J., Ma, T., Wang, M., Wu, Q.L., 2012. Diversity analysis of bacterial community compositions in sediments of urban lakes by terminal restriction fragment length polymorphism (T-RFLP). World J. Microbiol. Biotechnol. 28 (11), 3159–3170.